Level densities of ^{74,76}Ge from compound nuclear reactions

A. V. Voinov, T. Renstrøm, D. L. Bleuel, S. M. Grimes, M. Guttormsen, A. C. Larsen, S. N. Liddick, G. Perdikakis, A. Spyrou, S. Akhtar, N. Alanazi, K. Brandenburg, C. R. Brune, T. W. Danley, S. Dhakal, P. Gastis, R. Giri, T. N. Massey, Z. Meisel, S. Nikas, S. N. Paneru, C. E. Parker, and A. L. Richard

Phys. Rev. C **99**, 054609 — Published 8 May 2019

DOI: 10.1103/PhysRevC.99.054609

Level densities of ^{74,76}Ge from compound nuclear reactions

A.V. Voinov,[1,*] T. Renstrøm,[2] D.L. Bleuel,[3] S.M. Grimes,[1] M. Guttormsen,[2] A.C. Larsen,[2] S.N. Liddick,[4,5] G. Perdikakis,[6,5] A. Spyrou,[7,5] S. Akhtar,[1] N. Alanazi,[1,†] K. Brandenburg,[1] C.R. Brune,[1] T.W. Danley,[1] S. Dhakal,[1,‡] P. Gastis,[6] R. Giri,[1] T.N. Massey,[1] Z. Meisel,[1] S. Nikas,[6,§] S.N. Paneru,[1] C.E. Parker,[1,¶] and A.L. Richard[1,**]

[1]*Department of Physics and Astronomy, Ohio University, Athens, OH 45701, USA*
[2]*Department of Physics, University of Oslo, 0316, Oslo, Norway*
[3]*Lawrence Livermore National Laboratory, 7000 East Avenue, Livermore, CA 94551 USA*
[4]*Department of Chemistry, Michigan State University, East Lansing, MI 48824, USA*
[5]*National Superconducting Cyclotron Laboratory, Michigan State University, East Lansing, MI 48824, USA*
[6]*Department of Physics, Central Michigan University, Mount Pleasant, MI 48859, USA*
[7]*Department of Physics and Astronomy, Michigan State University, East Lansing, MI 48824, USA*

The level densities of ^{74,76}Ge nuclei have been studied with ^{68,70}Zn(^{7}Li, Xp) reactions. Proton evaporation spectra have been measured at backward angles in a wide energy region from about 2 to 25 MeV. The analysis of spectra allowed for a testing of level density models used in modern reaction codes for practical cross section calculations. Our results show that at excitation energies above the discrete level region, all level density models tested in this work overestimate the level densities that are needed to reproduce proton spectra from these reactions. The Gilbert and Cameron model, which includes the constant temperature energy dependence of the level density, shows the best agreement with experiment, however, its parameters need to be adjusted to reflect the observed reduction of the level density at higher excitation energies.

I. INTRODUCTION

Nuclear level densities have been of renewed interest in recent years due to their wide use in calculations of astrophysical phenomena, which often require a large number of nuclear reaction rates as input. The majority of nuclear reaction rates used in astrophysical reaction rate libraries, e.g. JINA REACLIB [1], BRUSLIB [2] are calculated using the Hauser-Feshbach reaction model [3], which needs nuclear level densities as input. Understanding these inputs is critical, as model calculations have indicated that nuclear reaction rate variations have a marked impact on a variety of phenomena, such as nucleosynthesis via the r-process [4], i-process [5], p-process [6], νp-process [7], and α-capture in neutron-rich ν-driven winds [8], as well as on the rp-process which powers X-ray bursts on accreting neutron stars [9]. Nuclear level densities are virtually unmeasured for nuclei off the valley of β-stability and Hauser-Feshbach (HF) models employing existing theoretical estimates already find a factor of 3 or more variability in resulting nuclear reaction rates [10, 11]. As such, nuclear level density measurements are critically needed to guide models.

Phenomenological level density models used in modern reaction codes are mainly based on Fermi-gas (FG) [12] or Gilbert and Cameron (GC) [13] prescriptions. The parameters such as the level density parameter a, the pairing shift Δ, the spin cutoff parameter σ, and the nuclear temperature T are found using experimental data on neutron resonance spacings [14] and the density of discrete low-lying levels known from spectroscopic experiments [15]. There are many different parameterizations developed to calculate the nuclear level density in a wide mass range. Some of them can be found in Refs. [13, 15–20]. The vulnerability of such an approach consists of the fact that neutron resonance spacings are known only for a very limited spin and excitation energy range. Such limitations might lead to uncertainties of calculated level densities in other spin and excitation energy ranges important for reaction cross section calculations. There are also uncertainties associated with analysis of neutron resonance data that requires accurate accounting for missing resonances, which is not always a straightforward procedure [15]. The experimental information on spin and parity distributions at excitation energies above the discrete level region is scarce and so an approach based on theoretical models is used. Therefore it is obvious that in order to progress further towards constraining level density models, other experimental data, beyond that on neutron resonance spacings, are needed.

The availability of microscopic level density calculations of the nuclear level density is also limited. The only global calculations for practical use are available in reaction codes such as Talys [21] and Empire [22]. These models are described in Refs. [23, 24]. Despite the fact that authors use a microscopic approaches, model

* voinov@ohio.edu
† Present address: Physics and Astronomy Department, King Saud University, 12371 Riyadh, Saudi Arabia
‡ Present address: Department of Physical Sciences Barry University, Miami Shores, Florida 33161
§ Present address: Institut fü Kernphysik (Theoriezentrum), Technische Universität Darmstadt, Schlossgartenstraße 2, D-64289 Darmstadt, Germany; GSI Helmholtzzentrum für Schwerionenforschung, Planckstrae 1, D-64291 Darmstadt, Germany
¶ Present address: Cyclotron Institute, Texas A&M University, College Station, Texas 77843, USA
** Present address: National Superconducting Cyclotron Laboratory, Michigan State University, East Lansing, MI 48824, USA

deficiencies are compensated with renormalization coefficients to match data on neutron resonance spacings and the density of discrete levels, the same way as phenomenological models do. There are calculations based on the shell model, such as the Shell Model Monte-Carlo approach used in Ref. [25]. However, calculations have been done for a very limited number of nuclei which do not include nuclei studied in this work.

The technique known as the Oslo method to obtain both the level density and the γ-strength function [26, 27] was initially based on measuring outgoing particle-γ coincidences with stable beams. It has now been expanded using β-radioactive nuclei produced with radioactive beams (it is referred to as the 'β-Oslo method' in the literature). The latter method uses the summing 4π detector SuN to detect γ-radiation following β-decay [28]. This technique is designed to constrain (n,γ) reaction rates in astrophysics for nuclei away from stability because the level density and the γ-strength functions are the most uncertain parameters determining (n,γ) cross sections. Both Oslo and β-Oslo methods use the simultaneous extraction of the level density and γ-strength functions from particle-γ (Oslo method) and $\beta-\gamma$ (β-Oslo method) coincidences. In order to get absolute values, extracted functions have to be normalized to absolute values available from other experiments. In most cases, again, the neutron resonance spacings and density of discrete levels are utilized.

The general question we address here is whether level density model parameterizations based on available neutron resonance spacing data are able to reproduce differential cross sections of nuclear reactions. This is a key question which needs to be addressed to understand the source of uncertainties of level density models used as inputs for cross section calculations. Specifically, it is important for low-energy reactions studied in astrophysics, including those occurring off the stability line. Since the experimental study of level densities off the stability line is currently very limited, the goal is to increase the accuracy of models by benchmarking them with an extended set of data, which would also include data from particle differential spectra of nuclear reactions. Studying different isotopes of the same element would help us to make more accurate extrapolations to the region off the stability line.

The purpose of this work is to use an experimental technique which would allow us to study the level density independently from data on neutron resonance spacings and in spin and excitation energy regions where resonance data are not available. Particle evaporation from compound nuclear reactions is a method which is known for its capability to study the nuclear level density [29], however, there is still a lack of analyses comparing level densities obtained from different experimental techniques. We found that the nuclei ^{74,76}Ge studied with Oslo [30] and β-Oslo [28] methods can be populated with the first stage (or primary) protons from the $^{68,70}\mathrm{Zn}(^{7}\mathrm{Li},\mathrm{p})^{74,76}\mathrm{Ge}$ reactions. First stage protons are

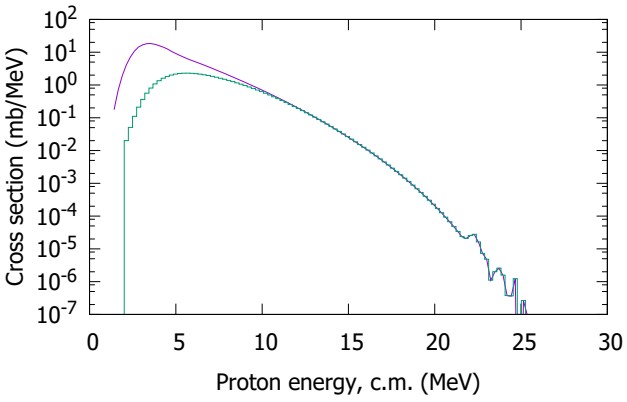

FIG. 1. Total $^{68}\mathrm{Zn}(^{7}\mathrm{Li},\mathrm{Xp})$ (full line) and primary $^{68}\mathrm{Zn}(^{7}\mathrm{Li},\mathrm{p})$ (histogram) proton evaporation spectra calculated with the Empire code [22] for the 16 MeV ^{7}Li projectiles.

protons that are the first particles emitted from a compound nucleus, as opposed to protons following other particles which come out first. The latter reactions are referred as $(^{7}\mathrm{Li},\mathrm{Xp})$ where X is any type and number of particles permitted by reaction Q-values. In the high energy region, a proton spectrum contains only primary protons populating levels from the ground state up to the lowest particle separation energy. The example of the first generated $^{68,70}\mathrm{Zn}(^{7}\mathrm{Li},\mathrm{p})^{74,76}\mathrm{Ge}$ and total proton spectra $^{68,70}\mathrm{Zn}(^{7}\mathrm{Li},\mathrm{Xp})^{74,76}\mathrm{Ge}$ calculated with the Empire code of Ref. [22] are shown in Fig 1.

If the energy of the lithium beam is low, slightly above the Coulomb barrier, it is expected that the compound mechanism is dominant and the differential cross section is determined by the evaporation reaction mechanism. In this case, according to the HF compound nuclear theory [3], both the differential cross sections and shape of the proton spectrum are determined by transmission coefficients of outgoing particles and the level density of the residual nuclei. It is assumed that transmission coefficients calculated from optical model potentials have much smaller uncertainties compared to level densities obtained from theoretical models (see Sec. IV for details). Therefore, particle evaporation spectra are used as a tool to test level density models.

In this work, proton spectra and corresponding differential cross sections are measured from the $^{70}\mathrm{Zn}(^{7}\mathrm{Li},\mathrm{Xp})$ as well as from $^{68}\mathrm{Zn}(^{7}\mathrm{Li},\mathrm{Xp})$ reactions. Proton spectra are compared with HF calculations using different level density model prescriptions. The level densities of both ^{74}Ge and ^{76}Ge are extracted from $^{68,70}\mathrm{Zn}(^{7}\mathrm{Li},\mathrm{p})^{74,76}\mathrm{Ge}$ primary proton spectra and compared with level densities obtained with the Oslo method [30] for ^{74}Ge, and with some theoretical models used as inputs for the reaction codes Talys [21] and Empire [22].

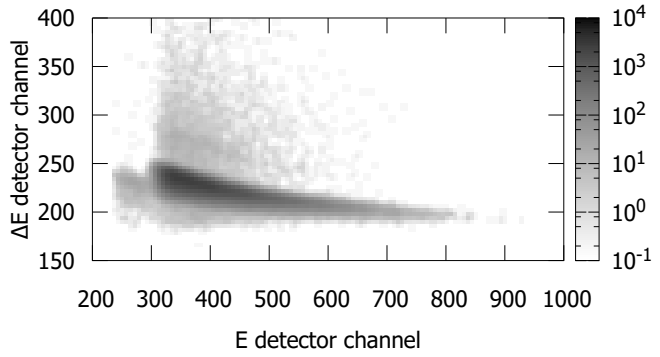

FIG. 2. Particle identification plot for the ΔE $-$ E telescope detector. The energy span for the E detector corresponds to the energy range between approximately 8 and 20 MeV.

II. EXPERIMENT

The experiment was performed at the Edwards Accelerator Laboratory [31] with the tandem electrostatic accelerator. A 16-MeV ^{7}Li beam was directed on a 3.5-mg/cm^2 ^{68}Zn and 4-mg/cm^2 ^{70}Zn metal foils enriched to 99.2% and 95.5%, respectively. Protons were registered with two methods. The first method used the time-of-flight technique. A Si detector was set-up at a distance of 1 m from the target at 142° with respect to the beam direction. Both time of flight and the energy deposited in the detector were used for particle identification. For this type of measurement the beam was pulsed and bunched with a repetition rate of 1.250 MHz and about 3 ns of a beam burst. With 1.5 mm thick Si detectors, protons were registered in the energy range of about 2-15 MeV. The second method used a $\Delta E - E$ telescope consisting of two 0.25 mm and 5 mm thick silicon detectors setup at minus 142° with respect to the beam direction and at distance of about 10 cm from the target. The direct current (DC) regime used for this method allowed us to increase the beam current considerably compared with the pulsed and bunched regime. Both DC beam and the short target-detector distance were indispensable to be able to acquire sufficient statistics for high energy protons, where the cross section drops exponentially as proton energy increases. Count rates were maintained at about 800 and 50 counts/sec for ΔE and E detectors respectively. The pile up effect was estimated with computer simulations and found to be negligible ($< 1\%$). The telescope was able to detect protons in the energy range from about 8 MeV to 25 MeV. Example of the particle identification plot (ΔE $-$ E) for the telescope detector is shown in Fig. 2. It shows no background in the high energy region, the low energy region contains some random background but its relative contribution was estimated to be less than one percent so its contribution was neglected Thus, the proton energy spectrum in the energy range from 2 to 25 MeV was obtained by combining the spectra from both time-of-flight and telescope detectors. The experimental energy resolution for protons in Si detectors was about 2%. The maximum energy of the outgoing protons in the laboratory system from these reactions is determined to be 24.06 MeV for the ^{68}Zn target and 24.36 MeV for the ^{70}Zn target. The energy calibration of the silicon detectors was determined from measurements of protons from ^{12}C(^{7}Li, p)^{18}O and ^{27}Al(^{7}Li, p)^{33}P reactions on thin natural carbon (about 0.05 mg/cm^2) and aluminum (about 0.7 mg/cm^2) foils. The first reaction gives a well characterized peak structure in the energy range 6-18 MeV due to population of discrete levels of ^{18}O. The second reaction allows us to use the similar structure at higher proton energies, around 22-25 MeV. This structure is due to population of discrete levels in ^{33}P. Since it was difficult to make calibration of ΔE and E detectors separately, the spectra measured by only E detector were used with non-linear calibration function. The calibrated proton spectra from reactions on carbon and aluminum are shown in Fig. 3. The same calibration was used for spectra measured from zinc targets. Because the large thicknesses of the zinc targets resulted in slowing down the lithium beam to about 13.5 MeV at the end of the target from its original 16 MeV, and because the reaction cross section decreases rapidly with the beam energy (see next section for details), the differential absolute proton yield $dY(\varepsilon_p)/d\varepsilon_p$ rather than the cross section $d\sigma(\varepsilon_p)/d\varepsilon_p$ was determined from this experiment. The uncertainty of the absolute proton yield is mainly determined by the uncertainties of the beam current integration (about 3 %) and detector solid angle (about 10 %). Experimental proton evaporation spectra from lithium induced reactions on both ^{68,70}Zn nuclei are shown in Fig. 4.

III. MODEL CALCULATIONS

The calculations of proton energy spectra have been performed with the reaction code Empire [22] using the HF model available as an option for compound reaction calculations. According to the HF theory, the energy-averaged cross section for the reaction with the projectile nucleus a and the ejectile b proceeding through states in a compound nucleus can be expressed as follows:

$$\frac{d\sigma}{d\varepsilon_b}(\varepsilon_a, \varepsilon_b) = \sum_{J\pi} \sigma^{\rm CN}_{J\pi}(\varepsilon_a) \frac{\sum_{I\pi} T_b(U, J, \pi, E, I, \pi)\rho_b(E, I, \pi)}{T(U, J, \pi)} \quad (1)$$

with

$$T(U, J, \pi) = \sum_{b'} \left(\sum_k T_{b'}(U, J, \pi, E_k, I_k, \pi_k) + \sum_{I'\pi'} \int_{E_c}^{U-B_{b'}} dE'\, T_{b'}(U, J, \pi, E', I', \pi')\, \rho_{b'}(E', I', \pi') \right) \quad (2)$$

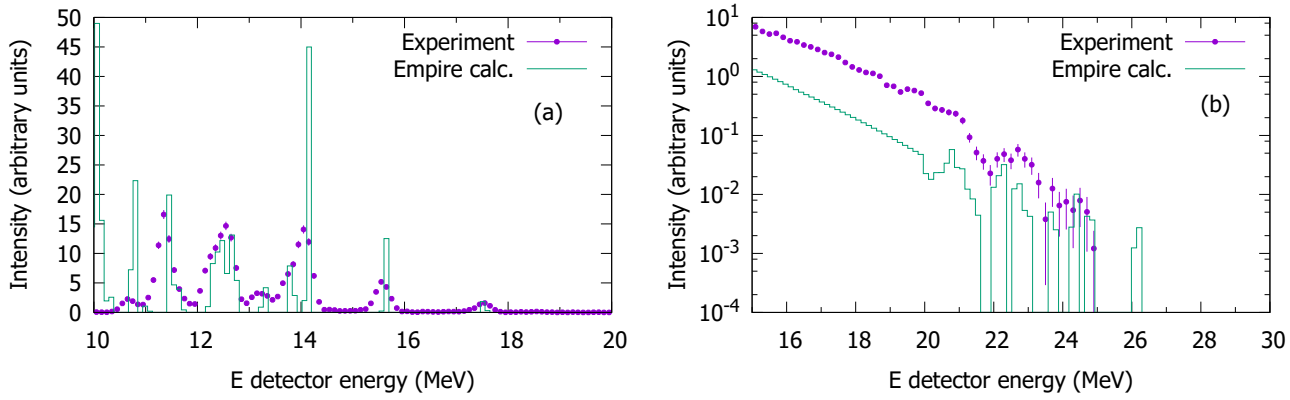

FIG. 3. Calibrated proton spectra from ^{12}C(^{7}Li, p) (a) and ^{27}Al(^{7}Li, p) (b) reactions measured by the E detector. Spectra are shown in the center of mass system. Empire calculations are arbitrary scaled to show the structure due to discrete level populations in residual nuclei. This structure was used for the energy calibration.

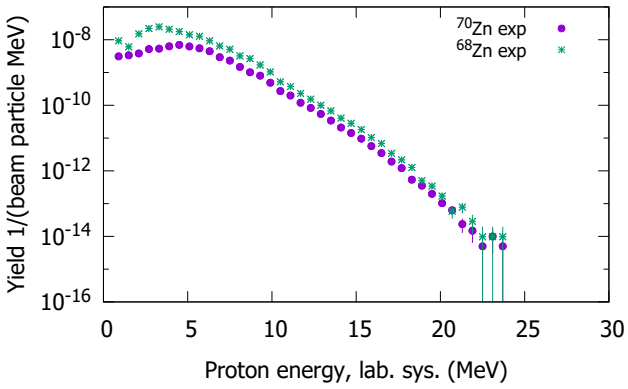

FIG. 4. Experimental proton evaporation spectra from ^{68,70}Zn(^{7}Li, Xp) reactions measured at 142°. Only statistical uncertainties are shown.

Here $\sigma^{CN}_{J\pi}(\varepsilon_a)$ is the fusion cross section, ε_a and ε_b are energies of relative motion for incoming and outgoing channels ($\varepsilon_b = U - E_k - B_b$, where B_b is the separation energy of particle b from the compound nucleus), the T_b are transmission coefficients of the outgoing particle, and the quantities (U, J, π) and (E, I, π) are the energy, the angular momentum, and the parity of the compound and residual nuclei, respectively. ρ_b is the level density of residual nuclei. The energy, E_c, is the discrete levels cut-off, above which the number of levels is calculated using a level density model. For energies below E_c, the known excitation energies E_k, spins, and parities of discrete levels are used. In practice, the E_c is already established in RIPL files [15] with discrete levels which are used as input files in Empire and Talys.

A. Fusion model

The HF formula (1) consists of two global terms, the first, $\sigma^{CN}_{J\pi}(\varepsilon_a)$, is a fusion cross section which is responsible for the formation of a compound nucleus and the second term determines its decay. The formation cross section determines the overall scaling of the double differential yield of outgoing particles. It also determines the J_π spin population in a compound nucleus. For light projectiles, the formation cross section is usually determined from optical model calculations, specifically from the imaginary potential of the optical model [22]. Optical model parameters are well established for light particles such as protons, neutrons, and to a lesser extent for α particles. For ^{7}Li projectiles, there is a compilation by J. Cook [32] but it does not include energies and nuclei of our interest. The optical parameters in Ref. [33] are established for ^{7}Li energies of about 30 MeV and higher. Therefore we used the coupled channel model available in the Empire code [22] as an option to calculate the fusion cross sections for projectiles heavier than α particles. Before this model was used in our calculations it was benchmarked against experimental fusion cross sections for the ^{7}Li + ^{64}Zn reaction from Ref. [34] in the energy region of our interest. The calculated fusion cross section is compared with experimental data in Fig. 5. A good agreement suggests the model is correct for fusion cross section calculations for our ^{7}Li+^{68,70}Zn reactions with 13.5-16 MeV (approximately 12.2-14.5 MeV in the center of mass (C.M.) system) for the projectile energy.

B. Test of level density models

We tested the following level density models which appear to be most distinct from each other because of different approaches that they use:

- the back-shifted Fermi-gas (referred to as

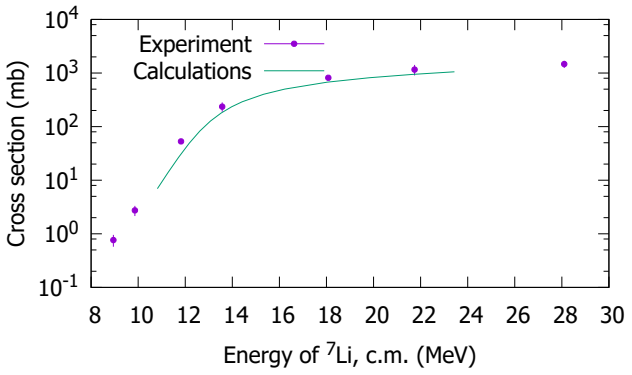

FIG. 5. Fusion cross section for ^{7}Li+^{64}Zn reaction. Data points are from Ref. [34]; the calculation is with the coupled channel model of the Empire code [22].

BSFG_RIPL_global) model based on Bethe formula [12]

$$\rho(U) = \frac{\exp(2\sqrt{aU})}{12\sqrt{2}\sigma a^{1/4}U^{5/4}}, \qquad (3)$$

where the effective excitation energy U is determined through the actual excitation energy E and the backshift parameter Δ as $U = E - \Delta$. The level density parameter a is determined to be energy dependent according to the Ignatyuk expression of Ref. [16]

$$a(U) = \tilde{a}\left[1 + \frac{\delta W}{U}\cdot(1 - exp(-\gamma\cdot U))\right], \qquad (4)$$

where $\tilde{a}$ is the asymptotic level density parameter, δW is the shell correction, and γ is the dumping parameter. Parameters are calculated according to the RIPL global systematics of Ref. [15]. The spin cutoff parameter, $\sigma(U)$, is determined according to the following expression:

$$\sigma^2(U) = 0.0138\cdot A^{5/3}\sqrt{U\cdot a(U)}/\tilde{a}. \qquad (5)$$

- the global parameterization of the Gilbert and Cameron model (GCM_RIPL_global) which is also based on prescriptions from the RIPL compilation [15]. The GC model combines the constant temperature and the Fermi-gas functions. At low excitation energies, below the matching energy $E < E_m$, the constant temperature formula is used:

$$\rho(E) = \frac{1}{T}\cdot\exp(\frac{E - E_0}{T}) \qquad (6)$$

The Fermi-gas model (3,4,5) is used for $E > E_m$.

- the back-shifted Fermi-gas parameterization according to Ref. [20] (referred as BSFG_Egidy09). It uses the model of Eq. (3) with the energy independent parameter a. Parameters a and Δ are obtained from fitting neutron resonance data and the density of discrete levels with Eq. (3) using a different spin cutoff formula which has been derived in Ref. [20] from fit to discrete levels with known spins only. Data on neutron resonances have not been used for the spin cutoff parameter derivation. The final formula was obtained to be as follows:

$$\sigma^2(E) = 0.391\cdot A^{0.675}\cdot(E - 0.5P_d)^{0.312}, \qquad (7)$$

where P_d is the deuteron separation energy. It suggests the spin cutoff parameter has a different excitation energy dependence (in power of 0.312 instead of 0.5) as it is prescribed in Eq. (5). It results in smaller level density parameters, a, leading to a flatter level density excitation dependence. It is expected that according to Eq. (1), it should also result in flatter proton evaporation spectra compared to those calculated with the spin cutoff model of Eq. (5).

- the microscopic calculations based on the Hartree-Fock-Bogoliubov (referred to as HFB 2008) combinatorial model allow calculations of parity and spin -dependent level densities [23]. This model is available as one of the input options in both the Empire and Talys computer codes. For practical calculations, the model uses renormalization coefficients to bring initial microscopical calculations into agreement with data on neutron resonance spacings and the density of discrete levels.

The zinc foils used as targets in the measurements were thick such that the interaction of projectiles with target nuclei occurred as projectiles slowed down from 16 MeV at the entrance to about 13.5 MeV at the exit of the target. According to Empire calculations, the fusion cross section decreases from 302 down to 42 mb in this energy range (see Fig. 5). In order to calculate a proton spectrum, the target was subdivided into slices, each one corresponded to the 0.5 MeV beam energy loss along the beam path. For each slice, the decrease of both the beam energy and fusion cross section were taken into account, and the corresponding proton spectrum was calculated with the Empire program in units of absolute proton yield $dY(\varepsilon_p)/d\varepsilon_p$. Each proton spectrum, initially calculated in the center-of-mass system, was converted to the lab system using reaction kinematics formulas and then all spectra were summed to get the final proton spectrum in the lab system. This approach allows us to make a comparison between experimental and calculated spectra for thick targets in the lab system.

The comparison between calculated and experimental proton spectra measured at 142° is shown in Fig. 6. One can see that the different model predictions result in more than an order of magnitude difference in proton yield, especially at higher proton energies. Generally, this indicates that the method based on experimental particle

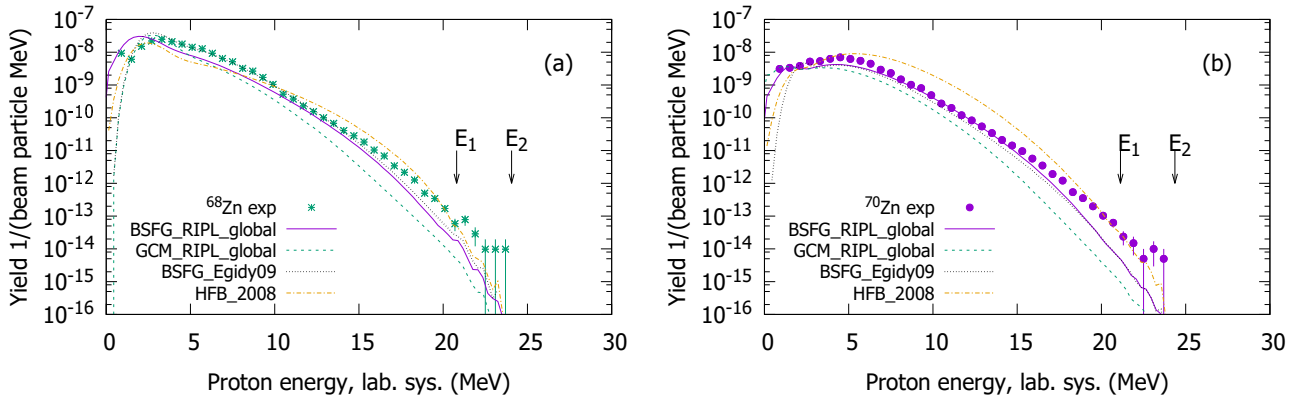

FIG. 6. Proton evaporation spectra from ^{68}Zn(^{7}Li, Xp) (a) and ^{70}Zn(^{7}Li, Xp) (b) reactions. Points are from this experiment, and are the same as in Fig 4, lines are calculations. Arrows show the energy interval where known discrete levels are used in calculations instead of level density models.

evaporation spectra is a good tool to benchmark level density models. Besides comparing absolute yields, it is also informative to compare shapes of spectra. As follows from the HF formula (1), the shape of a proton spectrum is mainly determined by the shape (functional dependence) of the level density of nuclei populated in this reaction, especially, the level density of the final nuclei populated by primary protons; in our case these are ^{74}Ge and ^{76}Ge from ^{68}Zn(^{7}Li, p)^{74}Ge and ^{70}Zn(^{7}Li, p)^{76}Ge reactions, respectively. It is seen from Fig. 6 that all calculations are unable to reproduce the shape of experimental proton spectra in the whole energy region. The common feature of all calculations is the rapid decrease of cross sections at higher proton energies, which is not supported by the data points. This indicates that the level density functions used in HF calculations are too steep for both ^{74}Ge and ^{76}Ge. This can be caused by the overestimation of the parameter a in the Fermi-gas level density formula (3) used in calculations. Because level density parameters for all models are based on neutron resonance data, this discrepancy might indicate some general problem in applying this parameterization to describe particle spectra from nuclear reactions, at least in some regions of the nuclear chart.

To verify that a decrease of the level density parameter $\tilde{a}$ in Eq. (4) would help us to reproduce experimental spectra, we implemented calculations in which $\tilde{a}$ was gradually decreased with the multiplication factor $m = (1.0 - 0.02n)$ where $n = 0, 1, 2, 3...$ and for each modified $\tilde{a}_{mod}$=$m\tilde{a}$, a calculated proton spectrum was compared to the experimental one by calculating the average relative deviation per experimental point

$$RD = \frac{1}{N}\sum_{i=1}^{i=N} \frac{\left| \frac{dY^i(E_p)}{dE_p}^{exp} - \frac{dY^i(E_p)}{dE_p}^{th} \right|}{\frac{dY^i(E_p)}{dE_p}^{exp}} \qquad (8)$$

in the proton energy range from 3 to 24 MeV. The values of the $\tilde{a}$ parameter were decreased globally for all nuclei populated in these reactions including those populated by (^{7}Li, n), (^{7}Li, np), and (^{7}Li, αp) decay channels. The best fit calculated spectra, which correspond to the minimum RD values obtained at $m \approx 0.82$ for the GCM_RIPL_global model, are compared with our data in Fig. 7. The comparison indicates a good agreement. The best fit obtained with the BSFG_RIPL_global model is shown for ^{70}Zn(^{7}Li, Xp) only for comparison (m=1). It underestimates data points at higher proton energies. Such analysis is considered to be approximation only, just to show in which direction models need to be modified. The specific values of parameters and their systematic uncertainties require deeper analysis that is beyond the scope of this paper.

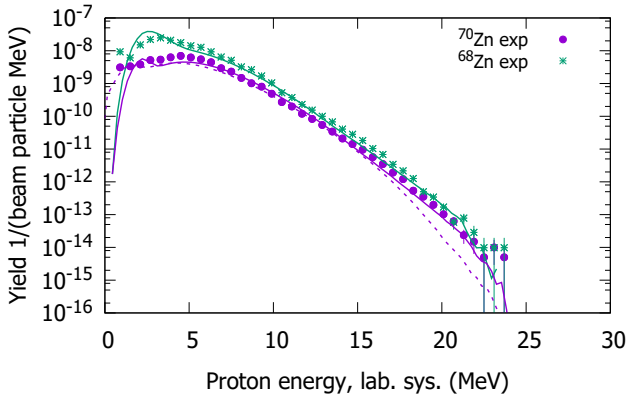

FIG. 7. Proton evaporation spectra from ^{68,70}Zn(^{7}Li, Xp) reactions. Points are experiment, same as in Fig 4, full lines are best fit calculations with GCM_RIPL_global level density model of Ref. [15] with the reduced level density parameter $\tilde{a}$. The dotted line is the best fit calculation with the BSFG_RIPL_global model for ^{70}Zn(^{7}Li, Xp). See text for details.

C. Pre-equilibrium mechanism

Since it is important to be confident that we consider proton spectra from purely compound reactions, the possible non-compound contributions which are presumably due to the pre-equilibrium reaction mechanism were estimated with the reaction code Empire. The code includes the module PCROSS which is based on the exciton model of Ref. [35] but has been developed further as described in Ref. [22]. Corrections due to pairing nuclear interactions were turned off, just to see an effect, otherwise, the pre-equilibrium contribution comes out to be almost negligible. The GCM_RIPL_global level density model with initial parameters of the RIPL-3 systematics [15] was used. The proton spectrum ^{68}Zn(^{7}Li, Xp) calculated with the pre-equilibrium reaction mechanism is compared with the compound spectrum in Fig. 8. The figure indicates that the pre-equilibrium contribution increases the proton cross sections in the energy range from 10 to 20 MeV and it rapidly decreases at higher energies so that it almost does not affect the high energy part of the proton spectrum. Experimental spectra do not exhibit such a signature, so that including the pre-equilibrium mechanism in calculations makes agreement with the shape of experimental spectra worse in the higher energy region and does not help us to explain the discrepancy between experimental and model proton spectra shown in Fig. 6. Calculations were done for the angle integrated spectrum. Calculating angular dependence is not implemented in the Empire code. It is expected that at backward angles the contribution from non-compound mechanisms is much smaller. In the next sections, the pre-equilibrium contribution is assumed to be negligible when the level density for both ^{74,76}Ge is extracted.

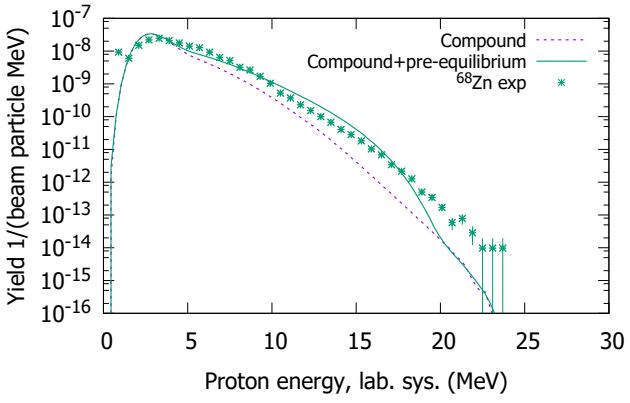

FIG. 8. Proton evaporation spectra from ^{68}Zn(^{7}Li, Xp) calculated with the Empire reaction code using the GCM_RIPL_global model. Lines show spectra calculated with the compound reaction model (dotted magenta line) and compound plus pre-equilibrium models (solid green line).

IV. UNCERTAINTIES DUE TO PROTON TRANSMISSION COEFFICIENTS

The HF Eq. (1) shows that both shape and absolute cross sections in proton spectra, besides level densities, also depend on transmission coefficients of outgoing particles, which in our case, are protons. Transmission coefficients are calculated from the optical model of nuclear reactions [36]. Most of the optical model parameters available in the literature are compiled in the RIPL data base [15]. For protons, there are seven different compilations applicable in our mass and energy ranges (see Table I). Proton spectra from ^{68}Zn(^{7}Li, Xp) were calculated with different optical model parameters from those compilations. Calculations performed for two level density models are presented in Fig. 9. It shows that the ratio for each level density model, between highest to lowest cross sections is a factor of about 2 in the lower energy region and it gradually reduces to about 15% (±7.5% from average) for higher proton energies. One can see that uncertainties due to uncertainties in proton transmission coefficients are much smaller in the high energy region than uncertainties due to different level density models.

TABLE I. References to proton optical model parameter compilations tested in calculations.

RIPL Ref. No.	4100	4101	5100	5405	5410	5501	5602
Reference	[37]	[38]	[39]	[40]	[41]	[42]	[43]

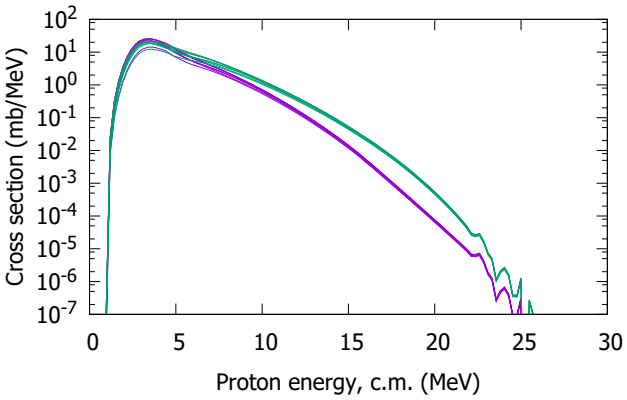

FIG. 9. Proton spectra from ^{68}Zn(^{7}Li, Xp) calculated with the HF model of the Empire [22] reaction code using GCM_RIPL_global (bottom lines) and BSFG_RIPL_global (top lines) level density models. The ^{7}Li beam energy is 16 MeV. There are seven lines for each level density models on the plot which show spectra calculated with seven different optical model parameterizations referenced in Table I.

V. LEVEL DENSITIES FOR ^{74,76}Ge

It was shown in the previous section that the level density parameter $\tilde{a}$ of the GCM_RIPL_global systematics based on neutron resonance data has to be reduced by about 20% to reproduce experimental proton evaporation spectra. In this section we attempt to estimate the actual level density functions for both ^{74,76}Ge in the excitation energy region which is populated by primary protons. According to model estimation shown in Fig. 1, the primary protons dominate for energies higher than about 12 MeV, corresponding to populating an excitation energy range up to about 13 MeV in a residual nucleus.

The technique is described in Ref. [29] and it was used in our previous publications [44–47]. It is based on the kinematics relation between the energy of the outgoing proton, ε_p, the excitation energy E^*_{res} of the residual nucleus $A-1$, and the Q-value of reaction

$$E_{cm} + (Q - E^*) = \varepsilon_p \cdot \frac{A-1}{A} + E_{res} \cdot \frac{1}{A}, \qquad (9)$$

where E_{cm} is the energy of the projectile in the center of mass system, E_{res} is the kinetic energy of the residual nucleus, and A is the atomic mass of the compound nucleus. The experimental level density function $\rho(E^*)_{exp}$ of the residual nucleus $A-1$ can then be obtained by binwise renormalization of the input level density function $\rho(E^*)_{\rm calc}$ used in calculations of $(Y(\varepsilon_p)/d\varepsilon)_{calc}$ as

$$\rho(E^*)_{exp} = \rho(E^*)_{\rm calc} \frac{(dY(\varepsilon_p)/d\varepsilon_p)_{\rm exp}}{(dY(\varepsilon_p)/d\varepsilon_p)_{\rm calc}} \cdot K_{norm}, \qquad (10)$$

where K_{norm} is a normalization coefficient calculated as a ratio of spectra integrals in the high energy region between E_1 and E_2, where primary protons populate discrete levels, i.e. where the density of levels is known:

$$K_{norm} = \frac{\left(\int_{E_1}^{E_2} dY(\varepsilon_p)/d\varepsilon_p \cdot d\varepsilon_p \right)_{calc}}{\left(\int_{E_1}^{E_2} dY(\varepsilon_p)/d\varepsilon_p \cdot d\varepsilon_p \right)_{\rm exp}}. \qquad (11)$$

The energy region corresponding to discrete level population is shown in Fig. 6 by arrows. Note, that Eq. (10) can only be used in the ε_p energy region where primary protons emitted from a compound nucleus dominate. This is usually valid in the high energy region which corresponds to excitation energies up to the neutron separation energy in a residual nucleus. Generally, such a technique does not allow for obtaining the absolute normalization of $\rho(E^*)_{exp}$ unless experimental data on $(dY(\varepsilon_p)/d\varepsilon_p)_{\rm exp}$ are available in the high energy ε_p region corresponding to population of discrete levels in a residual nucleus. In this case the absolute normalization becomes possible using information about the density of discrete levels from the level scheme and applying the normalization coefficient of Eq. (11). In this work, difficulty arises from the large target thickness that causes the experimental proton spectra to be a sum of spectra resulting from different ^{7}Li beam energies due to the slowing down of the beam in the target. Therefore, it is not possible to establish one-to-one correspondence between the energy ε_p of an outgoing proton and the excitation energy E^*_{res} of the residual nucleus populated by this proton as it follows from Eq. (9). The lithium beam loses about 2.5 MeV in the target. For this reason, as a first approach, we used an approximation that consists of using $(Y(\varepsilon_p)/d\varepsilon_p)_{calc}$ in Eq. (10) to be an average spectrum calculated at an average lithium beam energy of 15 MeV (instead of the actual 16 MeV) which was calculated as an average of beam energies weighted with the fusion cross sections while the beam passes through the target. The level density functions extracted using approach are shown by points in Figs. 10-12. For the second approach, we used Eqs. (9-11) to extract a set of 15 level densities for ^{74}Ge and ^{76}Ge. For different level densities in each set, the same experimental $(dY(\varepsilon_p)/d\varepsilon_p)_{\rm exp}$ proton spectrum was used but the calculated $(dY(\varepsilon_p)/d\varepsilon_p)_{\rm calc}$ was different corresponding to a different projectile energy as the projectile slows down in the target. The level densities were extracted with a 0.1 MeV projectile energy step in a 14 - 16 MeV energy interval. The $(^7{\rm Li}, {\rm p})$ cross section at 14 MeV is about 5% of the cross section at the initial 16 MeV, so it is assumed that the remaining contribution has a negligible effect on the shape of the proton evaporation spectra. The variation between different extracted level densities in a set gives an estimation of uncertainties due to the large target thicknesses in our experiment. These uncertainties are shown in Figs. 11-12 by shaded bands which include statistical uncertainties as well. The GCM_RIPL_global model with adjusted parameters was chosen for $\rho(E^*)_{\rm calc}$ in (10) since it was shown in Fig. 7 that it allows one to reproduce experimental spectra sufficiently well.

Comparison with level density models used for proton spectra calculations presented in Fig. 6 is shown in Fig. 11. The comparison shows that all models have a much steeper excitation energy dependence compared to experimental data points and this is the reason for the discrepancy between the calculated and experimental proton spectra in Fig. 6. Such a discrepancy implies an overestimation of the level density for model predictions at higher energies. It appears that level density models which are parameterized with available data on neutron resonance spacings are not able to reproduce experimental proton differential cross sections from compound reactions due to an overestimation of the level densities at higher excitation energies.

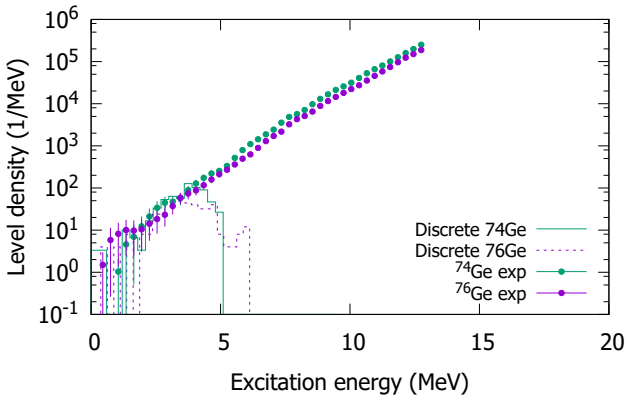

FIG. 10. Experimental level densities for ^{74,76}Ge extracted assuming the average 15 MeV ^{7}Li beam energy (see text for details).

.

Comparison with data obtained from the Oslo technique

The level density for ^{74}Ge has been studied in Ref. [30]. ^{3}He $-\gamma$ coincidences from the reaction of ^{74}Ge(^{3}He,^{3} He$'\gamma$) were analyzed with the Oslo method. The procedure of the level density extraction has been performed and the level density was normalized using the density of discrete levels at low-excitation energies and the density of neutron resonances at the neutron separation energy of 10.192 MeV. The same level density model from Ref. [20] which is referred to as BSFG_Egidy09 in this work, was also used to estimate the total density of levels at the neutron separation energy. The comparison with the data of this work (referenced as Ohio data) obtained from the proton evaporation spectrum is presented in Fig. 12. The figure indicates that agreement is quite good up to about 6 MeV in excitation energy and data start to diverge at higher energies. One should understand, however, that the normalization procedure in the Oslo level density requires an independent estimate of the absolute total level density at some excitation energy. Usually this estimate is based on the model for the spin and parity distribution at the neutron separation energy and on neutron resonance spacing data. Incorrect estimates of any or all of these would result in an incorrect estimation of the total level density used for normalization of the Oslo data points. Therefore, the discrepancy in Fig. 12 reflects the fact that the spin distribution model and neutron resonance data at the neutron separation energy for ^{74}Ge result in the total level density estimate to be higher than that obtained from the Ohio experiment. This is also shown in Fig. 11 where the BSFG_Egidy09 model overestimates data points by a factor of about 2. It is obvious from Fig. 12 that normalizing Oslo data points to data points from the Ohio experiment would bring level densities to a good agreement.

The level density for ^{76}Ge was obtained with the β-Oslo method in Ref. [28]. Data points were deduced at excitation energies below 3 MeV where discrete levels are known and data points from our experiment have large uncertainties (see Fig. 10). All data and models in this energy region agree within uncertainties. Nevertheless, a strong indication of this work that at higher excitation energies theoretical level density models parameterized with neutron resonance data might not be consistent with level densities estimated from particle spectra, needs to be taken into account when estimating the absolute level density and γ-strength functions with the Oslo method.

VI. DISCUSSION

It is important to note that experimental proton spectra obtained in this work are distinct from most of the similar spectra available from literature in a way that protons were measured in a wide energy region spanning from 2 to 25 MeV which includes protons populating discrete states at low excitation energies of residual nuclei. Such spectra are very sensitive to the level density of populated nuclei. Availability of data points corresponding to the population of discrete levels allows one to estimate absolute values of level density functions.

It appears that proton spectra measured in this work are totally due to the compound reaction mechanism because of the following considerations: they were measured at backward angles and the possible contributions due to the pre-equilibrium reaction mechanism, which is an usual concern in such types of experiments, were estimated with the exciton model in the Empire code [22] and found to be inconsistent with experimental data points. We do not exclude, however, that the pre-equilibrium model can be modified so it would be able to reproduce the high energy part of the experimental proton spectra with available level density models. This is a subject for future developments of nuclear reaction models. For the moment it is shown that only the reduction of level densities at higher energies allows one to describe experimental proton spectra well.

Two other possible effects, which could, in principle, explain the high energy increase of proton spectra have also been considered. The first one is the pile-up effect, when two consecutive pulses from a detector overlap and are registered as a single proton with a higher energy. The second effect is when two protons from (^{7}Li, pp) reaction channel are registered by one detector at the same time. The pile-up effect was estimated in section II and found to be negligible. According to Empire calculations, the cross section of the (^{7}Li, pp) channel constitutes of about $5 \cdot 10^{-4}$ from the cross section of the (^{7}Li, p) channel. Considering that the probability of registering two protons simultaneously by the same detector is about 10^{-6} at our geometry, this effect can be neglected as well.

All level density models currently used as input options in reaction codes are parameterized using the data on neutron resonance spacings, which are usually believed

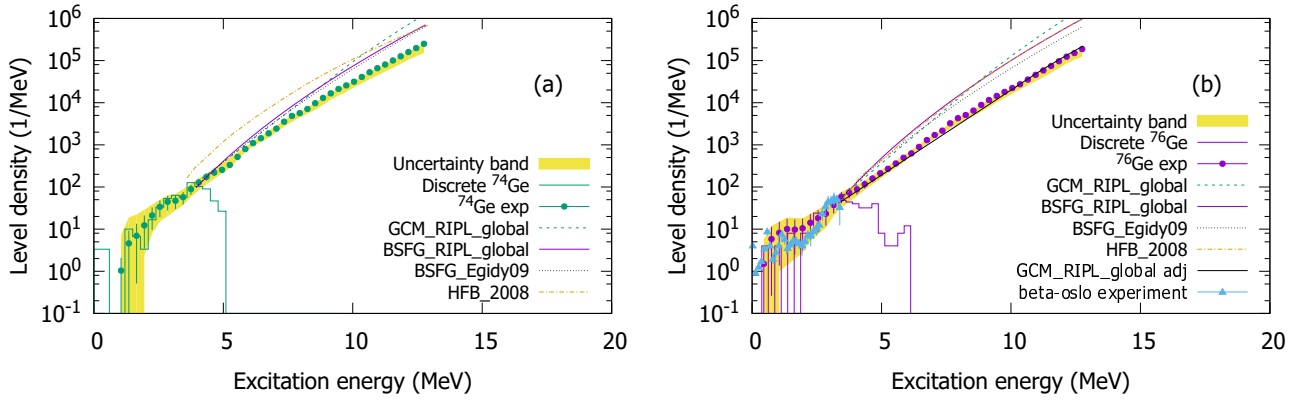

FIG. 11. Experimental (same as in Fig. 10) and model level densities for ^{74}Ge (a) and ^{76}Ge (b). The "GCM_RIPL_global adj" on the right panel shows the GCM_RIPL_global level density model calculated with the parameter $\tilde{a}$ adjusted (reduced) to fit the experimental proton spectrum from the ^{70}Zn(^{7}Li, Xp) reaction as it is shown in Fig. 7. Shaded bands include both the statistical uncertainties and the uncertainties resulting from the large target thicknesses (see text for details).

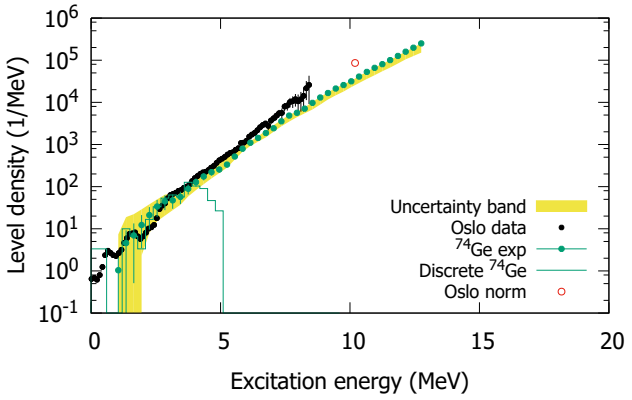

FIG. 12. Comparison between ^{74}Ge level densities estimated from proton evaporation spectra of the Ohio experiment (same as in Figs. 10-11) and from analysis of the Oslo experiment from Ref. [30].

to be the only reliable data on level densities at the neutron separation energy. Even microscopic calculations of Ref. [23] use renormalization coefficients to bring initially calculated level densities into agreement with neutron resonance data. The data obtained in this work might indicate that the level density models parameterized with neutron resonance data overestimate the absolute level densities at neutron separation energies and higher. Depending on the model, a factor in the range from 2.2 to 3.7 is obtained for the ^{74}Ge nucleus at the neutron separation energy of 10.196 MeV. More studies are needed to confirm this.

The inability of level density models to describe reaction differential cross sections of lithium induced reactions on ^{68,70}Zn isotopes raises the important general question of degree of applicability of models parameterized with neutron resonances to describe reaction cross sections. The main question is in which excitation energy and atomic mass region are such models applicable and where the disagreement can be observed. The available data and studies on this subject are scarce and not conclusive. The data obtained in this work might be the first indication of the problem. This should bring the focus on possible uncertainties of the level density model parameterizations, most uncertain of which are the spin and parity distribution models at the neutron separation energy. Also, some of the data on neutron resonance spacings might need to be revised. There is still a disagreement between different evaluations of the same data, specifically, for the ^{74}Ge nucleus studied here the values of the level spacings for s-wave resonances were reported to be 124(14) eV [48], 99(10) eV [14] and 62(15) eV [15]. The s-wave resonance spacing which would be consistent with our estimate of the level density function is around 200 eV. This estimate is based on existing models of gaussian spin distribution with the spin cutoff parameter according to Eq. (5). All possible uncertainties stemming from resonance data analysis might lead to an incorrect estimation of level density parameters in certain mass ranges. Therefore it is important to include other experimental data in the analysis, specifically evaporation spectra of compound nuclear reactions which are sensitive to the nuclear level density. On the other hand, there are needs for developments of nuclear reaction models, specifically correct estimates of contributions from pre-equilibrium and other non-compound reaction mechanisms for different types of projectiles, their energies and angular distribution of ejectiles.

VII. CONCLUSION

Proton differential cross sections from ^{68,70}Zn(^{7}Li, Xp) reactions have been studied with a 16-MeV ^{7}Li beam. Proton spectra were measured at the backward angle of 142° in the energy range from 2 to 25 MeV. Spectra were

analyzed with the HF compound nuclear reaction theory to test level density models for ^{74,76}Ge isotopes. Analysis shows that HF calculations with input level density models based on neutron resonance data are not able to reproduce experimental proton differential cross sections. Experimental data suggest that model level densities need to be reduced as the excitation energy increases in ^{74,76}Ge isotopes. This can be achieved if the asymptotic level density parameter $\tilde{a}$ in Eq. (4) is reduced by about 20% from that calculated with the systematics of Ref. [15]. The reduction of the level density parameter results in disagreement with data on neutron resonance spacings if the same form of the spin and parity distribution is used. This finding is considered to be important for further studies of level densities and their parameterizations in this and other mass ranges. Further studies need to be performed using an extended set of data including neutron resonances and particle evaporation spectra from compound reactions. It would allow better understanding spin and parity distributions of the level density and lead to increased accuracy of reaction cross section calculations for practical needs.

VIII. ACKNOWLEDGMENT

The authors thank accelerator engineers D. Jacobs and D. Carter for help with electronic setup and smooth operation of the accelerator. This work was supported in part by the U.S. Department of Energy, Grants No. DE-NA0002905, DE-SC0019042, DE-FG02-88ER40387, DE-NA-0003221, DE-NA-0003180 (NSSC), and DE-AC52-07NA27344. A.C.L. and T.R. gratefully acknowledge financial support through ERC-STG-2014 under grant agreement no. 637686, and from the ChETEC COST Action (CA16117), supported by COST (European Cooperation in Science and Technology).

[1] R. H. Cyburt, A. M. Amthor, R. Ferguson, Z. Meisel, K. Smith, S. Warren, A. Heger, R. D. Hoffman, T. Rauscher, A. Sakharuk, H. Schatz, F. K. Thielemann, and M. Wiescher, The Astrophysical Journal Supplement Series **189**, 240 (2010).
[2] Y. Xu, S. Goriely, A. Jorissen, G. L. Chen, and M. Arnould, A&A **549**, A106 (2013).
[3] W. Hauser and H. Feshbach, Phys. Rev. **87**, 366 (1952).
[4] M. Mumpower, R. Surman, G. McLaughlin, and A. Aprahamian, Progress in Particle and Nuclear Physics **86**, 86 (2016).
[5] P. Denissenkov, G. Perdikakis, F. Herwig, H. Schatz, C. Ritter, M. Pignatari, S. Jones, S. Nikas, and A. Spyrou, Journal of Physics G: Nuclear and Particle Physics **45**, 055203 (2018).
[6] W. Rapp, J. Grres, M. Wiescher, H. Schatz, and F. Käppeler, The Astrophysical Journal **653**, 474 (2006).
[7] C. Fröhlich and T. Rauscher, AIP Conference Proceedings **1484**, 232 (2012), https://aip.scitation.org/doi/pdf/10.1063/1.4763400.
[8] J. Bliss, A. Arcones, F. Montes, and J. Pereira, Journal of Physics G: Nuclear and Particle Physics **44**, 054003 (2017).
[9] R. H. Cyburt, A. M. Amthor, A. Heger, E. Johnson, L. Keek, Z. Meisel, H. Schatz, and K. Smith, The Astrophysical Journal **830**, 55 (2016).
[10] M. Beard, E. Uberseder, R. Crowter, and M. Wiescher, Phys. Rev. C **90**, 034619 (2014).
[11] J. Pereira and F. Montes, Phys. Rev. C **93**, 034611 (2016).
[12] H. A. Bethe, Phys. Rev. **50**, 332 (1936).
[13] A. Gilbert, F. S. Chen, and A. G. W. Cameron, Can. J. Phys **43**, 1248 (1965).
[14] S. F. Mughabghab, *Atlas of Neutron Resonances* (Elsevier, 2006).
[15] R. Capote, M. Herman, P. Obložinský, P. G. Young, S. Goriely, T. Belgya, A. V. Ignatyuk, A. J. Koning, S. Hilaire, V. A. Plujko, M. Avrigeanu, O. Bersillon, M. B. Chadwick, T. Fukahori, Z. Ge, Y. Han, S. Kailas, J. Kopecky, V. M. Maslov, G. Reffo, M. Sin, E. S. Soukhovitskii, and P. Talou, Nucl. Data Sheets **110**, 3107 (2009), `https://www-nds.iaea.org/RIPL-3`.
[16] A. V. Ignatyuk, G. N. Smirenkin, and A. S. Tishin, Sov. J. Nucl. Phys. **21**, 255 (1975).
[17] P. G. Young, Los Alamos National Laboratory Report LA-9468-PR (1984).
[18] A. Iljinov, M. Mebel, N. Bianchi, E. D. Sanctis, C. Guaraldo, V. Lucherini, V. Muccifora, E. Polli, A. Reolon, and P. Rossi, Nuclear Physics A **543**, 517 (1992).
[19] T. von Egidy and D. Bucurescu, Phys. Rev. C **72**, 044311 (2005).
[20] T. von Egidy and D. Bucurescu, Phys. Rev. C **80**, 054310 (2009).
[21] A. J. Koning, S. Hilaire, and M. C. Duijvestijn, in *Proceedings of the International Conference on Nuclear Data for Science and Technology (April 22-27, 2007, Nice, France)*, edited by O. Bersillon, F. Gunsing, E. Bauge, R. Jacqmin, and S. Leray (EDP Sciences, 2008) p. 211.
[22] M. Herman, R. Capote, B. Carlson, P. Obložinský, M. Sin, A. Trkov, H. Wienke, and V. Zerkin, Nucl. Data Sheets **108**, 2655 (2007).
[23] S. Goriely, S. Hilaire, and A. J. Koning, Phys. Rev. C **78**, 064307 (2008).
[24] S. Hilaire, M. Girod, S. Goriely, and A. J. Koning, Phys. Rev. C **86**, 064317 (2012).
[25] Y. Alhassid, M. Bonett-Matiz, S. Liu, and H. Nakada, Phys. Rev. C **92**, 024307 (2015).
[26] A. Schiller, L. Bergholt, M. Guttormsen, E. Melby, J. Rekstad, and S. Siem, Nucl. Instrum. Methods **A447**, 498 (2000).
[27] A. Voinov, M. Guttormsen, E. Melby, J. Rekstad, A. Schiller, and S. Siem, Phys. Rev. C **63**, 044313 (2001).
[28] A. Spyrou, S. N. Liddick, A. C. Larsen, M. Guttormsen, K. Cooper, A. C. Dombos, D. J. Morrissey, F. Naqvi, G. Perdikakis, S. J. Quinn, T. Renstrom, J. A. Rodriguez, A. Simon, C. S. Sumithrarachchi, and R. G. T. Zegers, Phys. Rev. Lett. **113**, 232502 (2014).

[29] H. Vonach, in *Proceedings of the IAEA Advisory Group Meeting on Basic and Applied Problems of Nuclear Level Densities, BNL Report No. BNL-NCS-51694*, edited by M. R. Bhat (Upton, Long Island, New York 11973, 1983) p. 247.

[30] T. Renstrøm, H.-T. Nyhus, H. Utsunomiya, R. Schwengner, S. Goriely, A. C. Larsen, D. M. Filipescu, I. Gheorghe, L. A. Bernstein, D. L. Bleuel, T. Glodariu, A. Görgen, M. Guttormsen, T. W. Hagen, B. V. Kheswa, Y.-W. Lui, D. Negi, I. E. Ruud, T. Shima, S. Siem, K. Takahisa, O. Tesileanu, T. G. Tornyi, G. M. Tveten, and M. Wiedeking, Phys. Rev. C **93**, 064302 (2016).

[31] Z. Meisel, C. Brune, S. Grimes, D. Ingram, T. Massey, and A. Voinov, Physics Procedia **90**, 448 (2017), conference on the Application of Accelerators in Research and Industry, CAARI 2016, 30 October 4 November 2016, Ft. Worth, TX, USA.

[32] J. Cook, Atomic Data and Nuclear Data Tables **26**, 19 (1981).

[33] B. Wang, W.-J. Zhao, E.-G. Zhao, and S.-G. Zhou, Phys. Rev. C **98**, 014615 (2018).

[34] A. Di Pietro, P. Figuera, E. Strano, M. Fisichella, O. Goryunov, M. Lattuada, C. Maiolino, C. Marchetta, M. Milin, A. Musumarra, V. Ostashko, M. G. Pellegriti, V. Privitera, G. Randisi, L. Romano, D. Santonocito, V. Scuderi, D. Torresi, and M. Zadro, Phys. Rev. C **87**, 064614 (2013).

[35] J. J. Griffin, Phys. Rev. Lett. **17**, 478 (1966).

[36] A. Bohr and B. R. Mottelson, *Nuclear Structure* (W. A. Benjamin, New York, 1969).

[37] F. G. Perey, Phys. Rev. **131**, 745 (1963).

[38] F. D. Becchetti and G. W. Greenlees, Phys. Rev. **182**, 1190 (1969).

[39] R. Varner, W. Thompson, T. McAbee, E. Ludwig, and T. Clegg, Physics Reports **201**, 57 (1991).

[40] A. J. Koning and J. P. Delaroche, Nucl. Phys. **A713**, 231 (2003).

[41] B. Morillon and P. Romain, Phys. Rev. C **76**, 044601 (2007).

[42] X. Li and C. Cai, Nuclear Physics A **801**, 43 (2008).

[43] E. S. Soukhovitski, S. Chiba, and J. Lee, AIP Conference Proceedings **769**, 1100 (2005), https://aip.scitation.org/doi/pdf/10.1063/1.1945199.

[44] A. V. Voinov, S. M. Grimes, C. R. Brune, M. J. Hornish, T. N. Massey, and A. Salas, Phys. Rev. C **76**, 044602 (2007).

[45] A. P. D. Ramirez, A. V. Voinov, S. M. Grimes, A. Schiller, C. R. Brune, T. N. Massey, and A. Salas-Bacci, Phys. Rev. C **88**, 064324 (2013).

[46] A. P. D. Ramirez, *Study of nuclear level density from deuteron induced reactions on* ^{54,56,58}*Fe, and* ^{63,65}*Cu*, Ph.D. thesis, Ohio University, Athens, Ohio (2014).

[47] Y. Byun, A. P. D. Ramirez, S. M. Grimes, A. V. Voinov, C. R. Brune, and T. N. Massey, Phys. Rev. C **90**, 044303 (2014).

[48] K. Maletski, L. B. Pikel'ner, I. M. Salamatin, and E. I. Sharapov, At Energy , 207 (2013).